Mathematical Medicine and Biology: A Journal of the IMA (2021) **00**, 1–17
doi:10.1093/imammb/dqab003

Models for plasma kinetics during simultaneous therapeutic plasma exchange and extracorporeal membrane oxygenation

Charles Puelz*
Department of Pediatrics, Section of Cardiology, Baylor College of Medicine and Texas Children's Hospital, Houston, TX, USA
*Corresponding author. Email: charles.puelz@bcm.edu

Zach Danial
Courant Institute of Mathematical Sciences, New York University, New York, NY, USA

Jay S. Raval
Department of Pathology, University of New Mexico, Albuquerque, NM, USA

Jonathan L. Marinaro
Department of Emergency Medicine, University of New Mexico, Albuquerque, NM, USA

Boyce E. Griffith
Departments of Mathematics, Applied Physical Sciences, and Biomedical Engineering, University of North Carolina; Carolina Center for Interdisciplinary Applied Mathematics, University of North Carolina; Computational Medicine Program, University of North Carolina, and McAllister Heart Institute, University of North Carolina, Chapel Hill, NC, USA

and

Charles S. Peskin
Courant Institute of Mathematical Sciences, New York University, New York, NY, USA

[Received on 10 June 2020; revised on 17 November 2020; accepted on 24 January 2021]

This paper focuses on the derivation and simulation of mathematical models describing new plasma fraction in blood for patients undergoing simultaneous extracorporeal membrane oxygenation and therapeutic plasma exchange. Models for plasma exchange with either veno-arterial or veno-venous extracorporeal membrane oxygenation are considered. Two classes of models are derived for each case, one in the form of an algebraic delay equation and another in the form of a system of delay differential equations. In special cases, our models reduce to single compartment ones for plasma exchange that have been validated with experimental data (Randerson *et al.*, 1982, *Artif. Organs*, 6, 43–49). We also show that the algebraic differential equations are forward Euler discretizations of the delay differential equations, with timesteps equal to transit times through model compartments. Numerical simulations are performed to compare different model types, to investigate the impact of plasma device port switching on the efficiency of the exchange process, and to study the sensitivity of the models to their parameters.

Keywords: compartment models; plasma kinetics; ECMO; delay differential equations; therapeutic plasma exchange.

1. Introduction

Therapeutic plasma exchange (TPE) refers to the removal and exchange of a patient's blood plasma. This procedure treats a variety of conditions, from renal diseases to neurological disorders (Chhibber & Weinstein, 2012; Madore *et al.*, 1996). It has very recently received attention as a possible therapy for COVID-19 (Dyer *et al.*, 2014; Keith *et al.*, 2020; Kesici *et al.*, 2020). TPE is typically done by connecting the patient's circulation to a device that slowly draws in blood, separates out old plasma, adds in new plasma or some other replacement fluid, and puts this mixture back into the native circulation. Extracorporeal membrane oxygenation (ECMO) is a procedure used for reoxygenating blood with an external circuit. There are two main types of ECMO, veno-venous and veno-arterial, and they are distinct from each other by virtue of the placement locations for the inlet and return lines within the patient's circulation (Pavlushkov *et al.*, 2017). Veno-venous ECMO (VV ECMO) draws from and replaces blood within the venous circulation. It is traditionally used when the patient's heart is functioning well enough to perfuse the organs. Veno-arterial ECMO (VA ECMO) bypasses both the heart and lungs and is used in cases where the patient needs both reoxygenation and circulatory support. In this case, blood is drawn from the veins and re-enters the native circulation through the arteries.

The clinical scenario of interest in this paper is simultaneous ECMO and TPE, which is usually done by connecting the TPE device directly to the ECMO circuit, often at the ECMO inlet line (Chong *et al.*, 2017; Jhang *et al.*, 2007; Laverdure *et al.*, 2018). This technique has been used to treat conditions such as multisystem organ failure or the rejection of a transplanted organ (Chong *et al.*, 2017; Jhang *et al.*, 2007; K Duan *et al.*, 2020). There are multiple parameters that affect the TPE procedure in these cases, including inlet and return flow rates for the ECMO and TPE devices, fraction of native cardiac output supported by the ECMO circuit, and recirculation of new plasma. This paper develops mathematical models that help quantify the impact of these parameters on plasma exchange done with ECMO. We derive two classes of models that each describe fraction of new plasma over time, and we consider both VV and VA ECMO. The approaches used in this paper can be applied to other apheresis techniques done in conjunction with ECMO.

To our knowledge there are no mathematical models for simulating simultaneous ECMO and TPE besides our previous work (Puelz *et al.*, 2020). This paper provides mathematical justification for our previous model, extends this approach to both VA and VV ECMO, and derives a new class of related models. There has been some research focused on separately modeling either TPE or ECMO procedures. A compartmental model of exchange kinetics was described by Kellogg & Hester (1988). They derived equations for plasma concentrations in both the intra- and extra-vascular spaces. A single compartment model for TPE was proposed by Randerson *et al.* (1982). Our approach is similar to the models introduced in these papers in that it describes plasma kinetics through several distinguished compartments, but our focus is on the interaction between the heart/lung, peripheral and ECMO compartments. When these compartments are considered together, we show that our model reduces to that of Randerson *et al.* (1982). Our approach is also able to describe possible recirculation of new plasma through these various spaces. As far as simulations for ECMO procedures, Zanella *et al.* (2016), used mathematical models for ECMO procedures to understand oxygenation in VV ECMO.

This paper provides derivations for two classes of models: algebraic delay equations (ADEs) and systems of delay differential equations (DDEs). We also consider two possible configurations for the TPE device, either 'typical' and 'switched'. These configurations refer to the orientation of the TPE device ports with respect to the ECMO device flow direction. In the typical configuration, the inlet line for the TPE device is upstream from the return line, and in the switched configuration these lines are reversed. A comparison of these two configurations was the focus of our initial modeling effort

TABLE 1 *A list of variables and their descriptions.*

Variable	Description
γ_1	New plasma fraction downstream from heart/lung compartment
γ_2	New plasma fraction downstream from peripheral compartment
$\tilde{\gamma}$	New plasma fraction downstream from ECMO compartment
$\hat{\gamma}$	New plasma fraction upstream from either the peripheral or heart/lung compartment

(Puelz *et al.*, 2020), and we further study these two configurations in this paper. We also present numerical results comparing different classes of models and different configurations of the TPE device.

2. Mathematical model descriptions

Our approach is to divide the system consisting of the patient, ECMO circuit, and TPE device into three compartments: (1) the heart and lungs, (2) the peripheral organs, and (3) the ECMO circuit with the attached TPE device. In our framework, the TPE device is not treated as a compartment but rather a source of new plasma and a sink for old plasma. Each compartment has an associated volume and flow rate of blood. The ratio of volume to flow determines the transit time of a parcel of new plasma through the given compartment. In particular, fixing two of the parameters for a given compartment (transit time, flow, or volume) will determine the third. Flows through compartments will always be specified, and either transit times or volumes will be given, depending on available data. Models are derived in this section for the typical and switched configurations in the cases of VA and VV ECMO with TPE. Tables 1 and 2 detail the variables and parameters used in our models.

In these models, Q is the volume of blood per unit time flowing through the peripheral compartment. The parameter α is defined so the product $\alpha\, Q$ is the flow through the ECMO compartment and by the TPE device. The parameter Q_1 is the flow into and out of the TPE device, which is typically much smaller than Q. In all cases, we assume the following constraints on α:

$$Q_1 < \alpha\, Q < Q. \tag{1}$$

See Fig. 1 for reference. These inequalities ensure that the flow into the TPE device does not exceed the flow going by it and that the ECMO device contributes a fraction α of the total cardiac output Q through the peripheral compartment. Define the parameter $[P]_0$ to be the volumetric concentration of total plasma (both new and old plasma) in blood, i.e. volume of plasma per volume of blood. We assume $[P]_0$ to be constant during the TPE process, and although it does not explicitly appear in the model equations, we use it for book keeping purposes in the derivation. The parameters s_1, s_2, and s_3 are transit times through the heart/lung, peripheral, and ECMO compartments, respectively. In practice, there are distributions of possible transit times, so these parameters can be interpreted as averages of these distributions. An interesting potential extension for these models would be to incorporate in some way the transit time distributions. The compartment blood volumes are V_1, V_2, and V_3. Volumes and transit times are related by the blood flow through each compartment, and these equations will be different in the cases of VA and VV ECMO.

Referring to Fig. 1, the variables of interest are $\gamma_1(t)$ and $\gamma_2(t)$, the fractions of new plasma in blood downstream from the heart/lung and peripheral compartments, respectively. Other auxiliary variables for fraction of new plasma in different locations of the models are used in the derivations and will

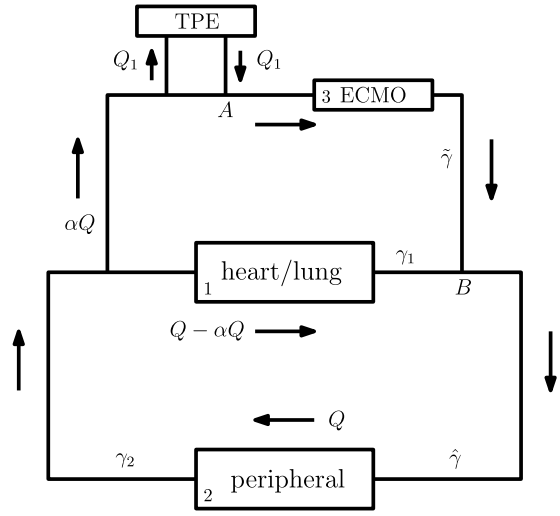

FIG. 1. The typical configuration for VA ECMO with TPE.

TABLE 2 *A list of parameters and their descriptions.*

Parameter	Description
Q_1	Flow into and out of the TPE device
Q	Flow through the peripheral compartment
α	Fraction of flow Q through the ECMO compartment
s_1	Transit time through heart/lung compartment
s_2	Transit time through peripheral compartment
s_3	Transit time through ECMO compartment
V_1	Volume of heart/lung compartment
V_2	Volume of peripheral compartment
V_3	Volume of ECMO compartment

be defined in context. We make two important simplifying assumptions that are used in the model derivation for each case. First, we assume old plasma is completely exchanged for new plasma, implying volume of old plasma per unit time flowing into the device and volume of new plasma per unit time flowing out of the device is $Q_1[P]_0$. A remark on incomplete plasma exchange is provided later in the paper. Second, we assume old and new plasma are instantaneously mixed at junctions. Under these assumptions, conservation of new plasma at junction A in Figs 1 and 2 is

$$\text{typical configuration, junction } A: \quad (\alpha Q - Q_1)\,\gamma_2(t - s_3)\,[P]_0 + Q_1\,[P]_0 = \alpha Q\,\tilde{\gamma}(t)\,[P]_0, \qquad (2)$$

in which $\tilde{\gamma}(t)$ is the fraction of new plasma directly downstream from the TPE device at time t. The first term in equation (2) also incorporates the transit time s_3 through the ECMO compartment as a delay. From this point forward, the model derivations for VA and VV ECMO are different and will be described in the following two subsections.

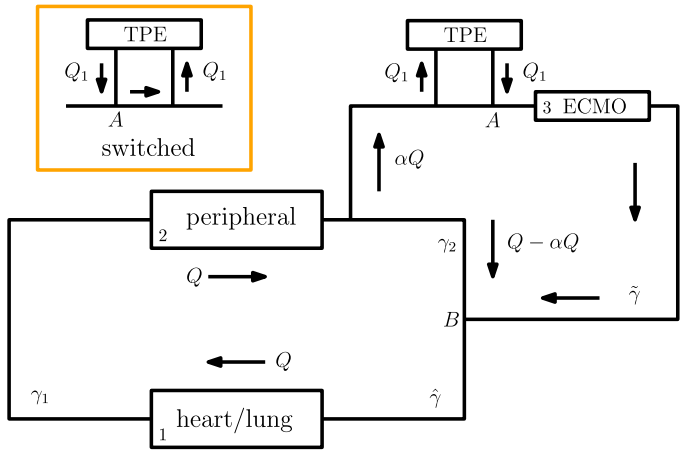

FIG. 2. Typical configuration for VV ECMO with TPE. The inset figure in the orange square shows the switched configuration of the TPE device as discussed in Subsection 2.3.

2.1 *The typical configuration for VA ECMO*

For the model of VA ECMO with TPE, as shown in Fig. 1, conservation of new plasma at junction B is

$$\text{junction } B: \quad \alpha Q\,\tilde{\gamma}(t)\,[P]_0 + (Q - \alpha Q)\,\gamma_1(t)\,[P]_0 = Q\,\hat{\gamma}(t)\,[P]_0, \tag{3}$$

where $\hat{\gamma}(t)$ is the fraction of new plasma directly upstream from the peripheral compartment. The transit times and volumes of the different compartments are related by the blood flows through each:

$$s_1 = \frac{V_1}{Q - \alpha Q}, \quad s_2 = \frac{V_2}{Q}, \quad s_3 = \frac{V_3}{\alpha Q}.$$

Two different models will be derived. The first model considers the change in volume of new plasma per unit time in the heart/lung and peripheral compartments:

$$\frac{d}{dt}(V_1\gamma_1) = (Q - \alpha Q)\,\gamma_2(t) - (Q - \alpha Q)\,\gamma_1(t),$$
$$\frac{d}{dt}(V_2\gamma_2) = Q\,\hat{\gamma}(t) - Q\,\gamma_2(t).$$

Using equations (2) and (3), we can rewrite these equations as a system of DDEs:

DDE model: typical configuration of VA ECMO with TPE

$$\begin{aligned}\frac{d}{dt}(V_1\gamma_1) &= (Q - \alpha Q)\,\gamma_2(t) - (Q - \alpha Q)\,\gamma_1(t),\\ \frac{d}{dt}(V_2\gamma_2) &= (Q - \alpha Q)\,\gamma_1(t) + Q_1 + (\alpha Q - Q_1)\,\gamma_2(t - s_3) - Q\,\gamma_2(t),\end{aligned} \tag{4}$$

which is our first model for the typical configuration of VA ECMO with TPE. An alternative model takes the form of an ADE. It is derived from equations (2)–(3) along with the following relationships between new plasma fractions at different locations and the transit times as delays:

$$\gamma_1(t+s_1) = \gamma_2(t) \quad \text{and} \quad \gamma_2(t+s_2) = \hat{\gamma}(t).$$

After algebraic manipulation, the equation for fraction of new plasma downstream from the heart/lung compartment is:

ADE model: typical configuration of VA ECMO with TPE

$$\gamma_1(t) = \frac{Q_1}{Q}\Big(1 - \gamma_1(t - s_2 - s_3)\Big) + \alpha\,\gamma_1(t - s_2 - s_3) + (1-\alpha)\,\gamma_1(t - s_1 - s_2). \tag{5}$$

2.2 *The typical configuration for VV ECMO*

Figure 2 depicts our model for VV ECMO with TPE. As in the previous section, we write down a statement for conservation of new plasma at junction B in Fig. 2:

$$\text{junction } B: \quad \alpha Q\,\tilde{\gamma}(t)\,[P]_0 + (Q - \alpha Q)\,\gamma_2(t)\,[P]_0 = Q\,\hat{\gamma}(t)\,[P]_0. \tag{6}$$

In this case, $\hat{\gamma}(t)$ is the fraction of new plasma upstream from the heart/lung compartment. As before, the transit times through the different compartments are determined by their volumes and corresponding flows:

$$s_1 = \frac{V_1}{Q}, \quad s_2 = \frac{V_2}{Q}, \quad s_3 = \frac{V_3}{\alpha Q}.$$

Conservation of new plasma through the peripheral and heart/lung compartments can be written in differential equation form as follows:

$$\begin{aligned}
\frac{d}{dt}(V_1\gamma_1) &= Q\,\hat{\gamma}(t) - Q\,\gamma_1(t),\\
\frac{d}{dt}(V_2\gamma_2) &= Q\,\gamma_1(t) - Q\,\gamma_2(t).
\end{aligned}$$

Using equations (2) and (6), we obtain a DDE model:

DDE model: typical configuration of VV ECMO with TPE

$$\begin{aligned}
\frac{d}{dt}(V_1\gamma_1) &= (Q - \alpha Q)\,\gamma_2(t) + Q_1 + (\alpha Q - Q_1)\,\gamma_2(t - s_3) - Q\,\gamma_1(t),\\
\frac{d}{dt}(V_2\gamma_2) &= Q\,\gamma_1(t) - Q\,\gamma_2(t).
\end{aligned} \tag{7}$$

An ADE can also be derived for this configuration using the following relationships between the transit times and new plasma fractions at different locations:

$$\gamma_1(t+s_1) = \hat{\gamma}(t) \quad \text{and} \quad \gamma_2(t+s_2) = \gamma_1(t).$$

After algebraic manipulation, we obtain:

ADE model: typical configuration of VV ECMO with TPE

$$\gamma_1(t) = \frac{Q_1}{Q}\Big(1 - \gamma_1(t - s_1 - s_2 - s_3)\Big) + \alpha\gamma_1(t - s_1 - s_2 - s_3) + (1 - \alpha)\gamma_1(t - s_1 - s_2). \quad (8)$$

In this case, the nonzero delay time s_3 for the ECMO compartment makes the models above much more interesting. If transport through the ECMO compartment occurs infinitely fast, i.e. $s_3 = 0$, both models (7) and (8) lose their dependence on α.

2.3 *Models for port switching within the TPE device*

Prior to initiating simultaneous TPE and ECMO, attachment of the inlet and return ports of the TPE device to the ECMO device is usually done in the typical vascular access configuration (see Fig. 2). In this typical configuration, the inflow port is upstream from the outflow port to avoid potential impacts of recirculation. However, in reality, there are often limitations in terms of availability of connections on the ECMO device tubing as well as safety issues surrounding the return of blood from the TPE device to sensitive points in the ECMO circuit that preclude connection via the typical vascular access configuration. In such cases, the risks of switching the TPE device ports and the resulting potential impacts of recirculation are outweighed by the benefits of a prompt and safe performance of TPE. The orange inset diagram in Fig. 2 depicts this switched vascular access configuration for VA and VV ECMO in which the inflow and outflow ports of the TPE device have been reversed from their typical configuration.

An application of this modeling approach will be the study of TPE device port switching on the efficiency of the TPE process. In this case, the inflow port is downstream from the outflow port, causing some recirculation of new plasma through the TPE device. The models for this scenario can be derived in the same way as for the typical configuration. The main difference in the derivation is the statement of conservation of new plasma at junction A:

$$\text{switched configuration, junction } A: \quad \alpha Q\,\gamma_2(t - s_3)\,[P]_0 + Q_1\,[P]_0 = (\alpha Q + Q_1)\,\tilde{\gamma}(t)\,[P]_0. \quad (9)$$

We remark that the reversal of TPE flow in the switched configuration leads to nontrivial differences between equations (2) and (9). In the typical configuration, the flow rate of new plasma from the TPE device, $Q_1[P]_0$, mixes with a new plasma flow of $(\alpha Q - Q_1)\,\gamma_2(t - s_3)\,[P]_0$. In the switched configuration, the TPE flow mixes with a new plasma flow of $\alpha Q\,\gamma_2(t - s_3)\,[P]_0$. For VA ECMO with TPE, we have the following DDE model:

DDE model: switched configuration of VA ECMO with TPE

$$\begin{aligned}
\frac{d}{dt}(V_1\gamma_1) &= (Q - \alpha Q)\,\gamma_2(t) - (Q - \alpha Q)\,\gamma_1(t),\\
\frac{d}{dt}(V_2\gamma_2) &= (Q - \alpha Q)\,\gamma_1(t) + \frac{\alpha Q\,Q_1}{Q_1 + \alpha Q} + \frac{\alpha^2 Q^2}{Q_1 + \alpha Q}\gamma_2(t - s_3) - Q\,\gamma_2(t).
\end{aligned} \quad (10)$$

The ADE model in this case is

ADE model: switched configuration of VA ECMO with TPE

$$\gamma_1(t) = \frac{\alpha Q_1}{Q_1 + \alpha Q}\Big(1 - \gamma_1(t - s_2 - s_3)\Big) + \alpha\,\gamma_1(t - s_2 - s_3) + (1 - \alpha)\,\gamma_1(t - s_1 - s_2). \tag{11}$$

For VV ECMO with TPE and the switched configuration for the ports, we have the following DDE model:

DDE model: switched configuration of VV ECMO with TPE

$$\begin{aligned} \frac{d}{dt}(V_1\gamma_1) &= (Q - \alpha Q)\,\gamma_2(t) + \frac{\alpha Q\,Q_1}{Q_1 + \alpha Q} + \frac{\alpha^2 Q^2}{Q_1 + \alpha Q}\gamma_2(t - s_3) - Q\,\gamma_1(t), \\ \frac{d}{dt}(V_2\gamma_2) &= Q\,\gamma_1(t) - Q\,\gamma_2(t). \end{aligned} \tag{12}$$

The ADE model for this case is

ADE model: switched configuration of VV ECMO with TPE

$$\gamma_1(t) = \frac{\alpha Q_1}{Q_1 + \alpha Q}\Big(1 - \gamma_1(t - s_1 - s_2 - s_3)\Big) + \alpha\gamma_1(t - s_1 - s_2 - s_3) + (1 - \alpha)\gamma_1(t - s_1 - s_2). \tag{13}$$

REMARK 1 Consider a special case for the models of VV ECMO with TPE in which the heart/lung and peripheral compartments are treated as a single compartment. In this case, assume the fractions of new plasma downstream from each of these compartments are the same:

$$\gamma_1(t) = \gamma_2(t).$$

Also, assume the transit time through the ECMO compartment is zero, corresponding to $s_3 = 0$. These assumptions formally convert our equations to those describing TPE within a single compartment. This single compartment model, described in detail by Randerson *et al.* (1982), has been used in calculations for TPE without ECMO, as described below.

Note that the DDE and ADE models for the typical configuration of VV ECMO with TPE do not depend on α. Interestingly, for the switched configuration, the models still depend on α. The DDE models for the typical and switched configurations of VV ECMO with TPE take the simplified form:

$$\frac{d}{dt}\gamma_2 = \frac{\beta}{V_1 + V_2}\left(1 - \gamma_2(t)\right), \tag{14}$$

where for the typical configuration we have $\beta = Q_1$ and for the switched configuration we have $\beta = \frac{\alpha Q\,Q_1}{\alpha Q + Q_1}$. Given the initial condition $\gamma_2(t = 0) = 0$ (corresponding to no new plasma at time $t = 0$), equation (14) for γ_2 has the following solution:

$$\gamma_2(t) = 1 - \exp\left(-\frac{\beta\,t}{V_1 + V_2}\right).$$

For the typical configuration, this equation can be rewritten as follows:

$$1 - \gamma_2(t) = \exp\left(-\frac{Q_1[P]_0 t}{(V_1 + V_2)[P]_0}\right). \tag{15}$$

The term $1 - \gamma_2(t)$ is the fraction of old plasma downstream from the heart/lung and peripheral compartments, at time t. The term $Q_1[P]_0\, t$ is the volume of plasma processed up to time t, since Q_1 is the TPE device flow, and $(V_1 + V_2)[P]_0$ is the total volume of plasma, both new and old, within the native circulation (i.e. the sum of volumes in the heart/lung and peripheral compartments). The ratio of these two terms appearing in the exponential of (15) can be interpreted as the number of plasma volumes processed, corresponding to a multiple of the total volume of plasma contained in the native circulation. In words, equation (15) is:

Typical Configuration

$$\begin{pmatrix} \text{fraction of old} \\ \text{plasma remaining} \end{pmatrix} = \exp\left(-\text{plasma volumes processed}\right), \tag{16}$$

which is one of the 'informal laws of apheresis'. Equation (16) is the same as that obtained in the single compartment model derived by Randerson *et al.* (1982), with the sieving coefficient of the TPE device equal to 1. This is significant since their model of TPE was validated with clinical data. The analogous equation for the switched configuration is:

Switched Configuration

$$\begin{pmatrix} \text{fraction of old} \\ \text{plasma remaining} \end{pmatrix} = \exp\left(-\frac{\alpha Q}{\alpha Q + Q_1} \times \text{plasma volumes processed}\right). \tag{17}$$

Equation (17) is slight modification of (16) and accounts for port switching in the TPE device; it includes the term $\frac{\alpha Q}{\alpha Q + Q_1}$ that multiplies the number of plasma volumes. Practically, the TPE device flow Q_1 is small relative to αQ, so the ratio $\frac{\alpha Q}{\alpha Q + Q_1} \approx 1$ and the typical and switched configurations have roughly the same exchange efficiency. As we shall show in our numerical results, the switched configuration is much less efficient in the regime $\alpha Q \approx Q_1$, i.e. when the ECMO device supports a small fraction of the cardiac output.

Remark 2 Our models assume complete exchange, implying the stream of fluid returning from the TPE device, with flow Q_1, contains 100% new plasma. This assumption can be relaxed by including an extra parameter $0 < \xi \leq 1$, defined to be the fraction of new plasma within the stream returning from the TPE device. The value $\xi = 1$ corresponds to complete exchange, and $\xi < 1$ corresponds to incomplete exchange. This parameter appears in the equation for conservation of new plasma at junction A, which in the typical configuration reads:

$$(\alpha Q - Q_1)\, \gamma_2(t - s_3)\, [P]_0 + \xi\, Q_1\, [P]_0 = \alpha Q\, \tilde{\gamma}(t)\, [P]_0.$$

The equation for the switched configuration is changed in a similar manner. These modified equations for junction A can be used to carry out the arguments in Remark 1 for the case of incomplete exchange.

The version of equation (14) that incorporates the parameter ξ is:

$$\frac{d}{dt}\gamma_2 = \frac{\beta}{V_1 + V_2}\left(\xi - \gamma_2(t)\right),$$

where β is the same as above for the typical and switched configurations. The analytical solution is:

$$\gamma_2(t) = \xi - \xi \exp\left(-\frac{\beta\, t}{V_1 + V_2}\right).$$

This solution results in a modified version of equation (16) for the typical configuration in the case of incomplete plasma exchange:

$$\begin{pmatrix} \text{fraction of old} \\ \text{plasma remaining} \end{pmatrix} = 1 - \xi + \xi \exp\left(-\text{plasma volumes processed}\right). \tag{18}$$

Equation (17) for the switched configuration is modified in the same way. Notice that for incomplete exchange corresponding to $\xi < 1$, equation (18) reveals the fraction of old plasma approaches $1 - \xi$ as the number of plasma volumes processed approaches infinity. This feature is consistent with the fact that the return stream from the TPE device has new plasma fraction ξ. In other words, regardless of the number of plasma volumes exchanged, the new plasma fraction cannot exceed ξ and the old plasma fraction cannot exceed $1 - \xi$.

Remark 3 The ADEs can be derived from the DDEs by replacing the time derivative with an approximate difference quotient. In particular, the difference quotient

$$\frac{d}{dt}(V_i\gamma_i) \approx \frac{V_i}{s_i}\left(\gamma_i(t + s_i) - \gamma_i(t)\right), \quad i = 1, 2, \tag{19}$$

used in the DDE model, combined with the relationships between the flows, volumes and transit times, results in the corresponding ADE model. As an example, equation (4) with approximation (19) becomes

$$\frac{V_1}{s_1}\left(\gamma_1(t + s_1) - \gamma_1(t)\right) = (Q - \alpha Q)\,\gamma_2(t) - (Q - \alpha Q)\,\gamma_1(t), \tag{20}$$

$$\frac{V_2}{s_2}\left(\gamma_2(t + s_2) - \gamma_2(t)\right) = (Q - \alpha Q)\,\gamma_1(t) + Q_1 + (\alpha Q - Q_1)\,\gamma_2(t - s_3) - Q\,\gamma_2(t). \tag{21}$$

Using $(Q - \alpha Q)\, s_1 = V_1$ in equation (20), we obtain the delay relation used to derive the ADE, namely,

$$\gamma_1(t + s_1) = \gamma_2(t).$$

The ADE (5) for this case follows from the above equation along with (21) and $Q\, s_2 = V_2$. Similar arguments can be made for the other configurations.

In this way, the ADE models can be interpreted as forward Euler discretizations of the DDE models, with timesteps equal to compartment transit times. Depending on the clinical scenario, TPE may be done multiple times, and each exchange procedure happens over the course of hours. The time scale of this process is slow in comparison to transit times through various compartments of the body. For example,

if the volume of blood is 5 L and the corresponding cardiac output is 5 L/minute, the transit time of a red blood cell through the entire circulation can be approximated as the ratio of volume to flow, i.e. 60 seconds. This separation of time scales reveals that the ADE and DDE models provide results very close to each other with a difference on the order of $\max(s_1, s_2)$.

3. Results

In this section, we describe some results from numerical simulations of our models for VA and VV ECMO with TPE. First, we compare the ADEs and DDEs. Second, we use these models to quantify the differences between the typical and switched configurations of the TPE device. Third, we perform an analysis of the sensitivity of these models to their parameters. All numerical computations are done in MATLAB (R2020b). In our simulations, the timestep size is chosen to be $\Delta t = 10^{-3}$ seconds. The transit times s_1, s_2 and s_3 are chosen in a manner to be described below based on parameters and other available data. They are selected to be the closest multiple of the timestep size for ease in simulating the models. The DDEs are discretized with the forward Euler method.

3.1 *Comparing algebraic delay and DDE models*

First, we compare the ADE and DDE models for each configuration. Nominal parameters are listed in Table 3 along with their references. The flow Q is set to 116.7 mL/second (Weiss, 2009). Transit times through the peripheral and heart/lung compartments are chosen to be $s_1 = 13$ seconds and $s_2 = 39$ seconds, following estimations of compartment volumes in Weiss (2009) and Niemann *et al.* (2002). We assume the ECMO circuit maintains 70% of the flow through the peripheral compartment corresponding to $\alpha = 0.7$ (Stevens *et al.*, 2017). The transit time through the ECMO compartment is determined by $s_3 = \frac{V_3}{\alpha Q}$, where the ECMO blood volume V_3 is chosen to be 500 mL (Belousova *et al.*, 2019; K Duan *et al.*, 2020). The TPE device flow Q_1 is set to 1.5 mL/second (Jhang *et al.*, 2007). Initial conditions for fractions of new plasma are $\gamma_1(t) = \gamma_2(t) = 0$ for $0 \leq t \leq s_1 + s_2 + s_3$.

Figure 3 shows a comparison of the ADE and DDE models for VA ECMO. The new plasma fraction downstream from the heart/lung compartment, $\gamma_1(t)$, is plotted for each case. Results for the typical configuration of the TPE device are on the left and results for the switched configuration are on the right. Figure 4 shows the corresponding results for VV ECMO. In both sets of figures, we included an inset figure which depicts a small subinterval of time to show the small differences between the ADE and DDE models. Following Remark 3, the two types of models are very close to each other since the compartment transit times are on the order of minutes, and the TPE procedure is simulated over the course of multiple hours. We also remark that the inset figures show some small differences between the typical and switched configurations. The switched configuration is less efficient since the fraction of new plasma at a given time is smaller than in the typical configuration. We further investigate these differences in the next subsection.

3.2 *The effect of port switching on TPE*

In this subsection, we use our models to compare the typical and switched configurations for the TPE device ports. In the switched configuration, the return line for the TPE device is upstream from the inlet line. This setup leads to recirculation of new plasma, meaning that some new plasma entering the ECMO circuit through the return line is immediately processed by the TPE device. The switched configuration is not an ideal setup for TPE, but our calculations in Remark 1 and simulations from the previous subsection suggest that it results in very similar exchange efficiency for a nominal choice

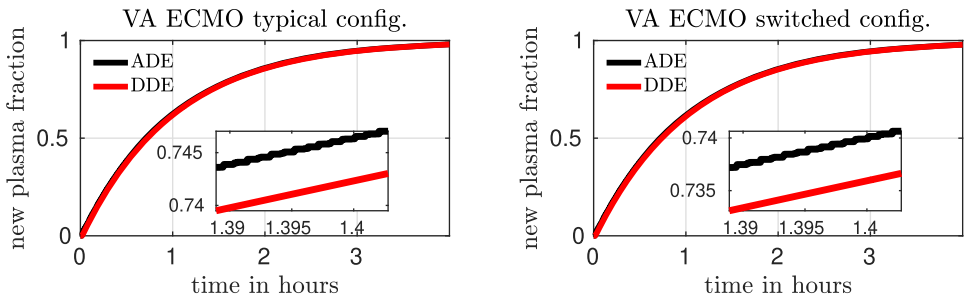

FIG. 3. A comparison of the ADE (black) and DDE (red) models for VA ECMO with TPE, for the typical configuration of the TPE on the left, and the switched configuration on the right. The inset figure shows a zoomed in portion of the results.

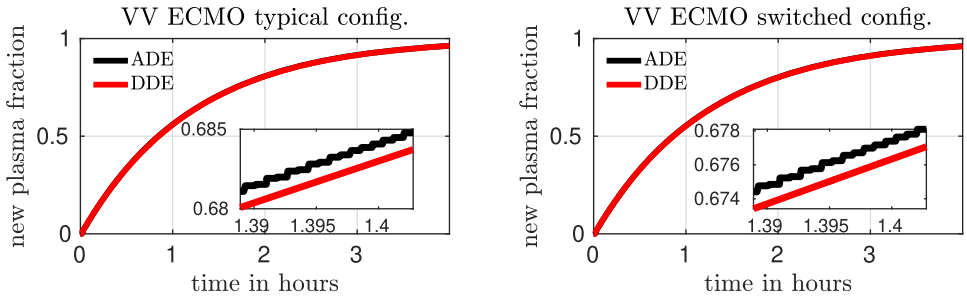

FIG. 4. A comparison of the ADE (black) and DDE (red) models for VV ECMO with TPE, for the typical configuration of the TPE on the left, and the switched configuration on the right. The inset figure shows a zoomed in portion of the results.

TABLE 3 *A list of nominal parameter values and corresponding references.*

Parameter	**Value**	**Reference(s)**
Q_1	1.5 mL/second	Jhang *et al.* (2007)
Q	116.7 mL/second	Weiss (2009)
α	0.7	Stevens *et al.* (2017)
s_1	13 seconds	Niemann *et al.* (2002); Weiss (2009)
s_2	39 seconds	Niemann *et al.* (2002); Weiss (2009)
V_3	500 mL	Belousova *et al.* (2019); K Duan *et al.* (2020)

of parameters. As also suggested in Remark 1, the switched configuration may be much less efficient when the fraction α of cardiac output supported by the ECMO device is very small. We point out that port switching has been shown to have a non-negligible effect in certain clinical scenarios where the stream of blood is accessed directly in a vein, instead of through the ECMO device (Level *et al.*, 2002; Twardowski *et al.*, 1993).

Figures 5 and 6 depict results from our models with smaller values of α and provide a comparison of the typical and switched configurations. Simulations are done with the DDE models and the same nominal parameters as in the previous section. In the left panel of these figures, we show new plasma fraction curves for both configurations and for the smallest value of α considered. The switched configuration for the cases of VA and VV ECMO is much less efficient in exchanging plasma than

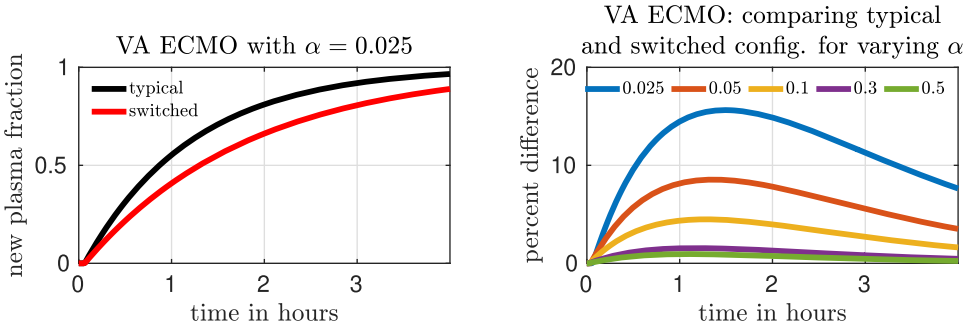

FIG. 5. Results for VA ECMO: the left panel shows fraction of new plasma for a small value of α for both the typical and switched configurations. The right panel shows the percent difference in fraction of new plasma between the typical and switched configurations for several values of α.

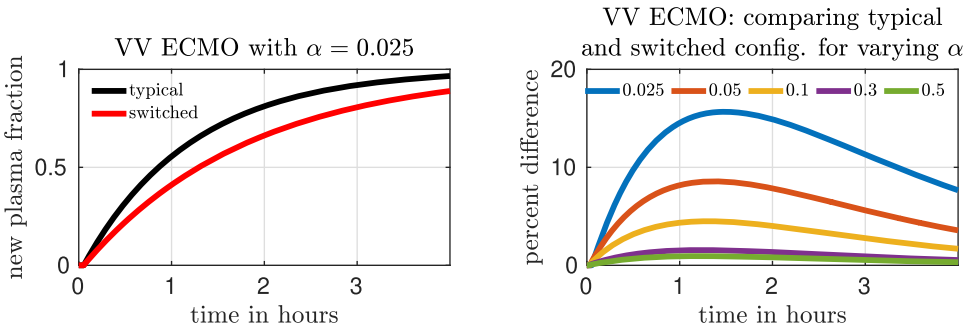

FIG. 6. Results for VV ECMO: the left panel shows fraction of new plasma for a small value of α for both the typical and switched configurations. The right panel shows the percent difference in fraction of new plasma between the typical and switched configurations for several values of α.

the typical configuration. The right panel shows percent differences between these configurations for different values of α. Notice that as α grows larger and closer to 1, both configurations maintain essentially the same exchange efficiency. These results indicate that for ECMO flows αQ close to the cardiac output Q and much larger than the TPE flow Q_1, the typical and switched configurations of the TPE device result in similar exchange efficiency. In contrast, if the fraction of cardiac output supported by the ECMO device is small, the switched configuration is nontrivially less efficient than the typical configuration.

3.3 *Sensitivity analysis*

This subsection describes a study of the sensitivity of the fraction of new plasma to changes in the parameters of the model. We define the sensitivity for a parameter $Y \in \{Q_1, Q, \alpha, s_1, s_2, V_3\}$ as the partial derivative of γ_1 with respect to Y, evaluated at $t = 2$ hours. The sensitivity is approximated as

$$\frac{\partial \gamma_1}{\partial Y}\Big|_{t=2 \text{ hours}} \approx \frac{\gamma_1(t, \tilde{Y}) - \gamma_1(t, Y)}{\tilde{Y} - Y}\Big|_{t=2 \text{ hours}},$$

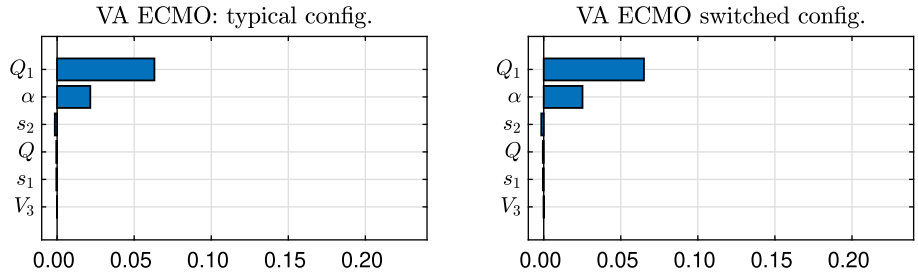

FIG. 7. Sensitivities for VA ECMO with the typical and switched configurations of the TPE device.

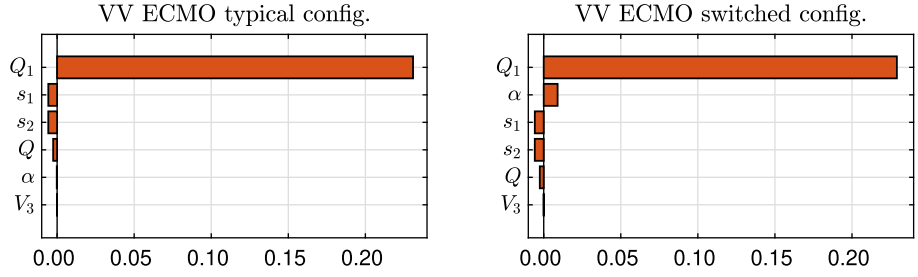

FIG. 8. Sensitivities for VV ECMO with the typical and switched configurations of the TPE device.

in which Y is taken to be the nominal value of the parameter used in Subsection 3.1, and $\tilde{Y} = 1.1 \times Y$, i.e. 10% larger than the nominal value. In other words, our approximation to the sensitivity is a forward difference approximation to the partial derivative. For calculations in this section, the DDE models for both the typical and switched configuration are used.

Figure 7 shows the sensitivities for the models of VA ECMO and for the typical and switched configurations of the TPE device in the left and right panels, respectively. Figure 8 shows the same results but for VV ECMO with TPE. Sensitivities are plotted on the same scale for comparison. The results reveal that for both types of ECMO and for the typical and switched configurations of the TPE device, Q_1 has the largest impact on the fraction of new plasma. Further, the TPE device flow is directly related to fraction of new plasma: an increase in Q_1 leads to an increase in new plasma fraction. Dependence on the flow Q_1 is shown in Fig. 9. This figure depicts new plasma fraction as a function of time for different values of Q_1. As expected, the new plasma fraction more quickly approaches 1 for larger values of Q_1. Another feature common across ECMO types and TPE device configurations is the lack of sensitivity with respect to the ECMO compartment volume V_3.

One puzzling aspect is the sensitivity of the models to the fraction α of cardiac output Q supported by the ECMO circuit. For VA ECMO and both TPE device configurations, an increase in α from its nominal value $\alpha = 0.7$, corresponding to an increase in ECMO circuit flow and hence flow by the TPE device, leads to an increase in the fraction of new plasma. This result is also seen for VV ECMO and the switched configuration of the TPE device. Surprisingly, the opposite result is seen for VV ECMO with the typical configuration of the TPE device: an increase in ECMO circuit flow results in very small drop in fraction of new plasma. This result is confirmed by Fig. 10, which depicts new plasma fraction evaluated at 2 hours for varying α and for both the typical and switched configurations.

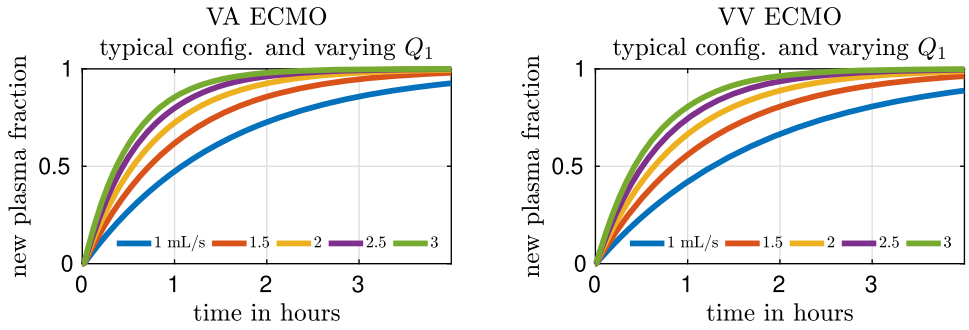

FIG. 9. New plasma fraction for the typical configuration of the TPE device with either VA (left panel) or VV (right panel) ECMO. The TPE flow Q_1 is varied from 1 mL/second to 3 mL/second. Note that as the flow Q_1 increases, the new plasma fraction approaches 1 more quickly.

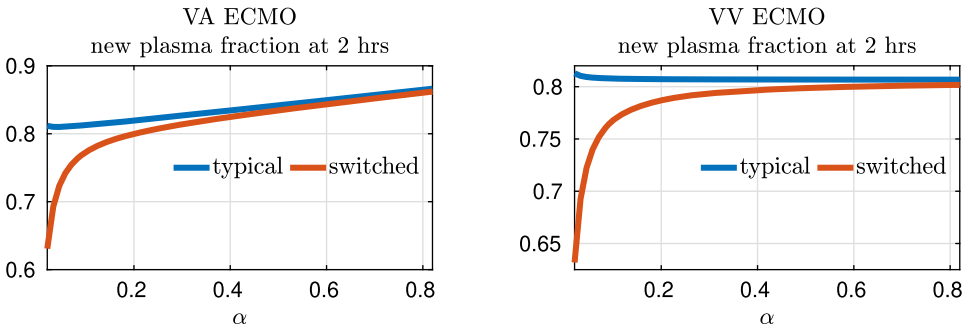

FIG. 10. New plasma fraction evaluated at 2 hours as the fraction of cardiac output α supported by the ECMO device varies.

Results for VA and VV ECMO are on the left and right panels, respectively, and are computed with the DDE formulation. For both ECMO types and the switched configuration, the new plasma fraction appears to be a monotone increasing function of α. For the typical configuration and VA ECMO, new plasma fraction is a decreasing function of α, but for larger α values, the new plasma fraction becomes monotone increasing. For the typical configuration and VV ECMO, the new plasma fraction varies little but does gradually decrease as α increases. An important takeaway from these results are the nontrivial differences between the typical and switched configurations for small fractions of cardiac output supported by the ECMO device. These differences suggest that TPE device port switching might have a detrimental effect on exchange efficiency in certain clinical scenarios that involve small flow rates through the ECMO device. We note that it was not possible to reach this conclusion in our initial modeling efforts because we did not describe the ECMO device as a separate compartment (Puelz *et al.*, 2020).

4. Conclusions

In this paper, we derived models for TPE done simultaneously with either VV or VA ECMO. These models describe fraction of new plasma in blood over time. Two types of models were developed: ADEs and systems of DDEs. We showed that our models in special cases reduce to the one described

by Randerson *et al.* (1982), which is important because their model was validated with clinical data. Our models extend their work by incorporating separate compartments for the native circulation and the ECMO device, and our models also account for recirculation of new plasma. We showed that the ADEs are forward Euler discretizations of the DDEs when the forward Euler timesteps are equal to compartment transit times. These transit times are small compared to the TPE procedure, so the ADEs and systems of DDEs gave very similar results. Our models were applied to the scenario of port switching in the TPE device, and our numerical results demonstrated that the switched configuration is less efficient in exchanging plasma when the ECMO flow is very small. Sensitivity analysis revealed the models are most sensitive to TPE device flow and least sensitive to ECMO circuit volume.

While a simplified version of our model can be compared to numerical and experimental data from Randerson *et al.* (1982), future work includes the procurement of clinical data from simultaneous ECMO and TPE procedures for validation. An important clinical application of our models is a study of port switching and its impact on exchange efficiency. Our results suggest that port switching has a small impact when the ECMO device supports most of the cardiac output. In contrast, when the ECMO device is supporting a small fraction of the cardiac output, port switching appears to have a non-negligible impact on exchange efficiency. This observation suggests that care must be taken when performing TPE through an ECMO circuit with small flows, like when a patient is being weaned off ECMO support. Our models can also be used for quantitative studies on the selection of device settings (flow rates and compartment volumes) for TPE and ECMO procedures. Each clinical scenario and patient is unique, and the impact of flow rates and compartment volumes for both the TPE and ECMO devices can be systematically studied using this framework.

Acknowledgements

This work was supported in part by the Research Training Group in Modeling and Simulation funded by the National Science Foundation via grant RTG/DMS-1646339.

References

Belousova, T., Tong, Y., Bai, Y., Klein, K., Tint, H. & Castillo, B. (2019) Utilization of therapeutic plasma exchange for hyperbilirubinemia in a premature newborn on extracorporeal membrane oxygenation. *J. Clin. Apher.*, **34**, 615–622.

Chhibber, V. & Weinstein, R. (2012) Evidence-based review of therapeutic plasma exchange in neurological disorders. *Seminars in Dialysis*, vol. 25. Wiley Online Library, pp. 132–139.

Chong, M., Lopez-Magallon, A. J., Saenz, L., Sharma, M. S., Althouse, A. D., Morell, V. O. & Munoz, R. (2017) Use of therapeutic plasma exchange during extracorporeal life support in critically ill cardiac children with thrombocytopenia-associated multi-organ failure. *Front. Pediatr.*, **5**, 254.

Dyer, M., Neal, M. D., Rollins-Raval, M. A. & Raval, J. S. (2014) Simultaneous extracorporeal membrane oxygenation and therapeutic plasma exchange procedures are tolerable in both pediatric and adult patients. *Transfusion*, **54**, 1158–1165.

Jhang, J., Middlesworth, W., Shaw, R., Charette, K., Papa, J., Jefferson, R., Torloni, A. S. & Schwartz, J. (2007) Therapeutic plasma exchange performed in parallel with extra corporeal membrane oxygenation for antibody mediated rejection after heart transplantation. *J. Clin. Apher.*, **22**, 333–338.

K Duan, B., Liu, C., Li, H., Zhang, T. Y., J Qu, M., Zhou, L., Chen, S., Meng, Y. H., et al. (2020) Effectiveness of convalescent plasma therapy in severe COVID-19 patients. *Proc. Natl. Acad. Sci. U. S. A.*, **117**, 9490–9496.

Keith, P., Day, M., Perkins, L., Moyer, L., Hewitt, K. & Wells, A. (2020) A novel treatment approach to the novel coronavirus: an argument for the use of therapeutic plasma exchange for fulminant COVID-19. *Crit. Care*, **24**. doi: https://doi.org/10.1186/s13054-020-2836-4.

Kellogg, R. M. & Hester, J. P. (1988) Kinetics modeling of plasma exchange: intra-and post-plasma exchange. *J. Clin. Apher.*, **4**, 183–187.

Kesici, S., Yavuz, S. & Bayrakci, B. (2020) Get rid of the bad first: therapeutic plasma exchange with convalescent plasma for severe COVID-19. *Proc. Natl. Acad. Sci. U. S. A.*, **117**, 12526–12527

Laverdure, F., Masson, L., Tachon, G., Guihaire, J. & Stephan, F. (2018) Connection of a renal replacement therapy or plasmapheresis device to the ECMO circuit. *ASAIO J.*, **64**, 122–125.

Level, C., Lasseur, C., Chauveau, P., Bonarek, H., Perrault, L. & Combe, C. (2002) Performance of twin central venous catheters: influence of the inversion of inlet and outlet on recirculation. *Blood Purif.*, **20**, 182–188.

Madore, F., Lazarus, J. M. & Brady, H. R. (1996) Therapeutic plasma exchange in renal diseases. *J. Am. Soc. Nephrol.*, **7**, 367–386.

Niemann, C. U., Yost, C. S., Mandell, S. & Henthorn, T. K. (2002) Evaluation of the splanchnic circulation with indocyanine green pharmacokinetics in liver transplant patients. *Liver Transpl.*, **8**, 476–481.

Pavlushkov, E., Berman, M. & Valchanov, K. (2017) Cannulation techniques for extracorporeal life support. *Ann. Transl. Med.*, **5**, 70. doi: 10.21037/atm.2016.11.47.

Puelz, C., Marinaro, J. L., Park, Y. A., Griffith, B. E., Peskin, C. S. & Raval, J. S. (2020) Mathematical modeling of the impact of recirculation on exchange kinetics in tandem extracorporeal membrane oxygenation and therapeutic plasma exchange. *J. Clin. Apher.*, **36**, 6–11. doi: https://doi.org/10.1002/jca.21805.

Randerson, D. H., Blumenstein, M., Habersetzer, R., Samtleben, W., Schmidt, B. & Gurland, H. J. (1982) Mass transfer in membrane plasma exchange. *Artif. Organs*, **6**, 43–49.

Stevens, M. C., Callaghan, F. M., Forrest, P., Bannon, P. G. & Grieve, S. M. (2017) Flow mixing during peripheral veno-arterial extra corporeal membrane oxygenation—a simulation study. *J. Biomech.*, **55**, 64–70.

Twardowski, Z. J., Van Stone, Jones, M. E., Klusmeyer, M. E. & Haynie, J. D. (1993) Blood recirculation in intravenous catheters for hemodialysis. *J. Am. Soc. Nephrol.*, **3**, 1978–1981.

Weiss, M. (2009) Cardiac output and systemic transit time dispersion as determinants of circulatory mixing time: a simulation study. *J. Appl. Physiol.*, **107**, 445–449.

Zanella, A., Salerno, D., Scaravilli, V., Giani, M., Castagna, L., Magni, F., Carlesso, E., Cadringher, P., Bombino, M., Grasselli, G., Patroniti, N. & Pesenti, A. (2016) A mathematical model of oxygenation during venovenous extracorporeal membrane oxygenation support. *J. Crit. Care*, **36**, 178–186.